



Self-steepening, Raman scattering and self-phase modulation-interactions via the perturbed Chen–Lee–Liu equation with an extra dispersion. Modulation instability and spectral analysis

H. I. Abdel-Gawad¹

Received: 6 March 2022 / Accepted: 22 April 2022 / Published online: 9 June 2022
© The Author(s) 2022

Abstract

It is worth mentioning that the perturbed Chen–Lee–Liu equation (PCLLE) exhibits the effects of self-steepening (SS), Raman scattering (RS) and self-phase modulation (SPM). Our attention is focused, here, to inspect the challenge between these phenomena may lead to a dominant one among them. On the other hand, we investigate the dominant phenomena produced due to these interactions. Furthermore, the structure of the configuration of pulses propagation in optical fibers are depicted. These phenomena are illustrated, here, via studying the PCLLE with an extra dispersion. This equation is formulated and the exact solutions of this new equation are found by using the unified method (UM). The importance of the UM stems from the fact that, in the applications, we have found that the UM is of low time cost in symbolic computation. So, we think that it prevails the known methods in the literature. On the other hand, the solutions for the complex envelope field equations, found in the literature, are always considered with real wave amplitude. Here, a transformation based on using complex wave amplitude is introduced. Indeed, in this case, solutions describe the waves that result from soliton- periodic wave collision, which may reveal novel phenomena. The solutions obtained are evaluated numerically and represented in graphs. It is shown that pulses compression occurs which may be due to self-phase modulation. Also, dispersive shock wave can be produced which may be argued to the presence of the extra dispersion and self-sdteepening. It is worthy to mention that, self-steepening arises for a small value of the related coefficient. The results obtained, here, are novel. The modulation instability is analyzed and it is found that it triggers at a critical values of SS and RS coefficients. At this stage, shock wave may occur. It is observed that the spectrum shows soliton with periodic waves background.

Keywords Chen–Lee–Liu equation · Self-steepening · Self-phase modulation · Modulation instability · Spectral analysis · Unified method

✉ H. I. Abdel-Gawad
hamdyig@yahoo.com

¹ Mathematics Department, Faculty of Science, Cairo University, Giza, Egypt

1 Introduction

The perturbed nonlinear Schrodinger equations, among them the PCLLE describes the propagation of optical pulses in optical fibers, retaining the interactions of self-steepening, Raman scattering and self phase modulation phenomena (Chen et al. 1979). In Chen et al. (1979) the inverse scattering method was used to study the integrability of nonlinear Hamiltonian systems. The PCLLE was currently studied in the literature. A generalized PCLLE with high nonlinearity perturbation terms were also considered. In this case, a PCLLE with taken full nonlinearity via integration algorithms, where solutions exhibit bright, dark, singular solitons were shown (Yıldırım et al. 2020). In Kudryashov (2019), the traveling wave reduction was used where two first integrals for the system of equations of the real and imaginary parts of the solution of PCLLE were found. A higher-order extension of the PCLLE with third-order dispersion and quintic nonlinearity terms was studied in Zhang et al. (2015) by constructing the n -fold Darboux transformation. By using modified $1/G'$ -expansion and modified Kudryashov methods, traveling wave solutions of PCLLE, where different aspects of the solutions produced by both analytical methods were discussed (Yokuş et al. 2021). Analytical bright soliton solutions, dark soliton solutions, periodic solutions of the fractional PCLLE were obtained by the modified $\exp(-\Omega(\xi))$ -expansion function method (Martínez et al. 2021). In Houwe et al. (2021), the chirped and the corresponding chirp with their stability to the PCLLE with self-phase modulation and nonlinear dispersions were presented. The Jacobi elliptic function technique was used to find solutions of PCLLE (Sarła et al. 2022). A novel modification for the generalized exponential rational function method was used to determine novel analytical solutions of PCLLE (Mohamed et al. 2022). The conservation laws of PCLLE in optical fibers together with the conserved densities were retrieved by Lie symmetry analysis (Karaa et al. 2018). The collective variable method to study two types of the CLLE, the classical and perturbed ones was employed (Alrashed et al. 2021). The classical Lie symmetry analysis was used to exhibit optical solitons to PCLLE (Bansal et al. 2020). Construction of different optical soliton solutions to the CLLE of monomode fibers, by executing the extended sinh-Gordon equation expansion method, logarithmic transformation, and the ansatz functions method, was executed (Bilal et al. 2021). The CLLE in birefringent fibers is examined to uncover dark, bright and also singular solitons (Yıldırım 2019). In Gaxiola and Biswas (2018), the CLLE in optical fibers was dealt with by the aid of Laplace Adomian decomposition method. The CLLE was investigated by the aid of fully shifted Jacobi's collocation method with two independent approaches, via discretization of the spatial variable and the temporal variable (Abdelkawy et al. 2021). Periodic wave trains of the CLLE evolved from fully developed modulation instability was found in Liu et al. (2021). Therein it was shown that a highly nontrivial spectral evolution of such waves leads to strong asymmetry of its components. The effect of fractional temporal evolution on chirped soliton solutions of the CLLE was studied by adopting the new modified sub-equation method to derive bright and dark solitons, periodic and singular function solutions (Dépélair et al. 2021). The classification of possible wave structures evolving from initially discontinuous profiles for the photon fluid propagating in a normal dispersion fiber was carried based on the generalized CLLE (Ivanov 2021). We mention that the PCLLE can be considered as kind of perturbed nonlinear Schrodinger equation (PNLSE), so that they may share many physical insights concerning the propagation of optical pulses in fiber optics. The PNLSE has received the attention of a variety of works. In Mihalache et al. (1993), the inverse scattering transform was used to find one-parameter and the breather-like four-parameter soliton solutions of a PNLSE.

The Riccati-Bernoulli Sub-ODE method was used to investigate exact wave solution of the PNLSE (Shehata 2016). In Mahak and Akram (2019), the extension of the rational sine-cosine method and rational sinh-cosh method to construct new exact solutions of PNLSE. The two $(G'/G, 1/G)$ -expansion methods were suggested to obtain abundant closed form wave solutions to the PNLSE and the cubic-quintic Ginzburg-Landau equation Miah et al. (2016). In Neirameh (2016), a new class of conformable fractional derivative for constructing new exact solitary wave solutions to the fractional PNLSE was proposed. New complex solitons to the PNLSE model with the help of an analytical method were obtained (Gao et al. 2020). In Zhang et al. (2010), the modified mapping method and the extended mapping method were used to derive some new exact solutions of the PNLSE. In the presence of parabolic law nonlinear fibers, Raman effect and self-steepening, the PNLSE was investigated using the sub-equation expansion method (Zhou 2014). The PNLSE was studied by utilizing two analytical methods, namely the extended modified auxiliary equation mapping and the generalized Riccati equation mapping methods (Osman et al. 2021). For the PNLSE, the exact traveling wave solutions, trigonometric, hyperbolic, rational, soliton and complex function solutions, via the extended (G'/G^2) -expansion method and the first integral method were obtained (Akram and Mahak 2018). An alternative method used to inspect the local and nonlocal integrability is the inverse scattering method was used employed in Ma (2022, 2021) and Ma and Yong (2021).

It is worthy to mention that, always in the literature, solutions of the NLSE, extended NLSE and Perturbed NLSE, for the complex envelope, were found by introducing real amplitude transformation. Very recently numerous works were carried by introducing complex amplitude transformation which inspect the waves that result from soliton-periodic wave collision. It reveals many new phenomena which were hidden in the traditional transformation (Abdel-Gawad 2012, 2021a, b, c, d, 2022; Abdel-Gawad et al. 2022; Tantawy and Abdel-Gawad 2020), and it is established that NLSE-type equations, they are integrable when the real and imaginary parts are linearly dependent. In the present work, we study the PCLLE in the presence of third order dispersion, where the interaction of self-steepening (SS), Raman scattering (RS) and self-phase modulation (SPM) is investigated, which is completely new. This is established by investigating the exact solutions of the PCLLE which are found by using the UM.

The outlines of this work are as follows.

In Sect. 2 the model equation and the method are presented. Section 3 is devoted to solutions in hyperbolic function forms. While, elliptic solutions are presented in Sect. 4. Modulation instability and the spectral analysis are studied in Sect. 5. Section 6 is devoted to conclusions.

2 The Model Eq. and outlines of the UM

2.1 The model Eq.

The propagation of optical pulses inside in a monomode fibers modeled by the CLL equation, which reads

$$iw_t + \alpha w_{xx} + \gamma |w|^2 w_x = 0, \quad (1)$$

where $w \equiv w(x, t)$ is the complex envelope field, α is the group dispersion velocity and γ is the coefficient of Raman scattering.

The perturbed Chen–Lee–Liu equation describe the propagation of optical pulses in plasma and optical fibers reads,

$$iw_t + \alpha w_{xx} + \gamma |w|^2 w_x = i[cw_x + \mu(|w|^2 w)_x + \sigma(|w|^2)_x w], \tag{2}$$

where c is the phase velocity, μ is the coefficient of self-steepening for short pulses and σ is the coefficient of self-phase modulation (nonlinear dispersion).

The PCLLE with high nonlinearity is,

$$iw_t + \alpha w_{xx} + \gamma |w|^2 w_x = i[cw_x + \mu(|w|^{2n} w)_x + \sigma(|w|^{2n})_x w], n > 1, n \in \mathbb{N}, \tag{3}$$

Here, we consider the Eq (2) with an extra dispersion,

$$iw_t + \alpha w_{xx} + i\beta w_{xxx} + \gamma |w|^2 w_x = i[cw_x + \mu(|w|^2 w)_x + \sigma(|w|^2)_x w], \tag{4}$$

where β is the coefficient of the highest order dispersion. We proceed by introducing a transformation with complex amplitude solution for $w(x, t)$ in the form,

$$w(x, t) = (u(x, t) + iv(x, t))e^{i(kx - \omega t)}, \quad w^*(x, t) = (u(x, t) - iv(x, t))e^{-i(kx - \omega t)}, \tag{5}$$

into (4), and the equations for the real and imaginary parts are given respectively by,

$$\begin{aligned} ku^3(\mu - \gamma) - v_t + u(ck - \alpha k^2 + \beta k^3 + kv^2(\mu - \gamma) + 2u_x v(\mu + \sigma) + \omega) \\ + v_x(c + 3\beta k^2 - 2\alpha k) + [u^2(\mu - \gamma) + v^2(-\gamma + 3\mu + 2\sigma)]v_x \\ + u_{xx}(\alpha - 3\beta k) - \beta v_{xxx} = 0, \end{aligned} \tag{6}$$

$$\begin{aligned} kv^3(\mu - \gamma) + u_t + [-c - 3\beta k^2 + 2\alpha k + u^2(\gamma - 3\mu - 2\sigma) \\ + v^2(\gamma - \mu)]u_x \\ + v(ck - \alpha k^2 + \beta k^3 + ku^2(\mu - \gamma) - 2u(\mu + \sigma)v_x + \omega) \\ + v_{xx}(\alpha - 3\beta k) + \beta u_{xxx} = 0. \end{aligned} \tag{7}$$

Here we use the transformations for the traveling wave solutions of (6) and (7), $u(x, t) = U(z)$, $v(x, t) = V(z)$, $z = hx + dt$, thus (6) and (7) reduce respectively to,

$$\begin{aligned} V'(-d + h(c + 3\beta k^2 - 2\alpha k) + hV^2(-\gamma + 3\mu + 2\sigma)) \\ + h^2(U''(\alpha - 3\beta k) - \beta hV^{(3)}) \\ + U(ck + 2hV(\mu + \sigma)U' - \alpha k^2 + \beta k^3 + kV^2(\mu - \gamma) + \omega) \\ + hU^2(\mu - \gamma)V' + kU^3(\mu - \gamma) = 0, \end{aligned} \tag{8}$$

$$\begin{aligned} U'(d - h(c + 3\beta k^2 - 2\alpha k) + hU^2(\gamma - 3\mu - 2\sigma)) \\ + h^2(\beta hU^{(3)} + V''(\alpha - 3\beta k)) \\ + V(ck - 2hU(\mu + \sigma)V' - \alpha k^2 + \beta k^3 + kU^2(\mu - \gamma) + \omega) \\ + hV^2(\gamma - \mu)U' + kV^3(\mu - \gamma) = 0. \end{aligned} \tag{9}$$

The exact solutions of (8) and (9) (or (6) and (7)) are obtained via the UM [1]. It asserts that the solutions of nonlinear partial differential equations are expressed in polynomial and rational forms, in an auxiliary function that satisfied an auxiliary equation.

2.2 Outlines of the UM

2.2.1 Polynomial forms

The solutions of (8) and (9) are written,

$$\begin{aligned}
 U(z) &= \sum_{j=0}^{j=n_1} a_j g(z)^j, & V(z) &= \sum_{j=0}^{j=n_2} b_j g(z)^j, \\
 (g'(z))^r &= \sum_{j=0}^{j=rk} c_j g(z)^j, & r &= 1, 2,
 \end{aligned}
 \tag{10}$$

where $g(z)$ is the auxiliary function together with the auxiliary equation (AE).

The polynomial solution (10) of (8) and (9) exists, in the sense of polynomial form, if there exist integers n_1, n_2 and k . To this issue, we analyze two conditions, the balance and consistency. We consider the case $r = 1$. With relevance to (8) and (9), the balance condition leads to $n_1 = n_2 = k - 1$. For the consistency condition we determine the number of equations that result from inserting (10) into these equations and by setting the coefficients of $g(z)^i, i = 0, 1, 2, \dots$ equal to zero (say $p(k) = 4k - 3$). Also, we determine the numbers of arbitrary parameters $\{a_j, b_j, c_j\}$ (say $q(k) = 2k - 1$). The condition for the existence of (10) reads $p(k) - q(k) \leq m$, m is the highest order derivative in (8) and (9). (here $m = 3$). We find that $1 \leq k \leq 7/2$, thus $k = 1, 2, 3$. The case when $r = 2$ is discussed by the same way. It is worth noticing that when $r = 1$ the solutions of (10) are hyperbolic functions, while when $r = 2$, they are periodic or elliptic functions.

2.2.2 Rational forms

In this case, for simplicity, we write directly,

$$\begin{aligned}
 U(z) &= \frac{a_1 g(z) + a_0}{s_1 g(z) + s_0}, & V(z) &= \frac{b_1 g(z) + b_0}{s_1 g(z) + s_0}, \\
 (g'(z))^r &= \sum_{j=0}^{j=rk} c_j g(z)^j, & r &= 1, 2.
 \end{aligned}
 \tag{11}$$

Indeed, rational solutions may be considered to describe “indirect” interactions, while (10) describes “direct” interactions. The discussion of existence of the rational forms is done by the same way as in the case of polynomial forms. Indeed the determination of the values k in (11) depends on the high nonlinearity and the highest order derivative in (8) and (9).

The importance of the unified method results from the fact that it is of low time cost in symbolic computations. Furthermore, it provides a wide class of solutions ranging from hyperbolic solutions, periodic solutions to elliptic solutions in Jacobi elliptic functions. So, think that it prevails the known methods in the literature.

3 Hyperbolic functions solutions of (8) and (9)

We consider the solution in (10) and find the polynomial and rational solutions.

3.1 Polynomial solutions

3.1.1 When $r = 1, k = 2$

Here, we write,

$$U(z) = a_1g(z) + a_0, \quad V(z) = b_1g(z) + b_0, b_0 = \frac{b_1}{a_1}a_0, \tag{12}$$

together with, the A E,

$$g'(z) = c_2g(z)^2 + c_1g(z) + c_0 \tag{13}$$

In (12) the real part and imaginary part are taken linearly dependent. By inserting (12) and (13) into (8) and (9) and by setting the coefficients of $g(z)^i, i = 0, 1, 2, ..$ equal to zero, we get,

$$\begin{aligned} \beta &= \frac{a_1^2(-\gamma)+3a_1^2\mu+2a_1^2\sigma-b_1^2\gamma+3b_1^2\mu+2b_1^2\sigma}{6c_2^2h^2}, \\ d &= \frac{\sqrt{a_1^2+b_1^2}(-6ck(\gamma+\sigma)(\mu+\sigma)+3\omega(\mu+\sigma)(\gamma-3\mu-2\sigma)+4ak^2(\gamma+\sigma)^2)}{9\sqrt{ac_2}\sqrt{k(\mu-\gamma)}\sqrt{\mu+\sigma}}, \\ c_0 &= \frac{1}{12c_2k(a_1^2+b_1^2)(\gamma-\mu)(\mu+\sigma)}(3a_1^2c_1^2k(\gamma-\mu)(\mu+\sigma)+3b_1^2c_1^2k(\gamma-\mu) \\ &\quad (\mu+\sigma)+2c_2^2(-6ck(\mu+\sigma)+\alpha k^2(\gamma+3\mu+4\sigma)-6\omega(\mu+\sigma))), \\ h &= \frac{\sqrt{k}\sqrt{a_1^2+b_1^2}\sqrt{\mu+\sigma}}{\sqrt{ac_2}}, \quad a_0 = \frac{a_1c_1}{2c_2}. \end{aligned} \tag{14}$$

The solution of (13) is,

$$\begin{aligned} g(z) &= \frac{1}{6c_2\sqrt{k}\sqrt{a_1^2+b_1^2}\sqrt{\mu+\sigma}}(3c_1\sqrt{k}\sqrt{a_1^2+b_1^2}(\gamma-\mu)\sqrt{\mu+\sigma}+ \\ &\quad \sqrt{6c_2}\sqrt{\gamma-\mu}\sqrt{6ck(\mu+\sigma)-\alpha k^2(\gamma+3\mu+4\sigma)+6\omega(\mu+\sigma)}) \\ &\quad \tanh\left(\frac{c_2(A_0+z)\sqrt{6ck(\mu+\sigma)-\alpha k^2(\gamma+3\mu+4\sigma)+6\omega(\mu+\sigma)}}{\sqrt{6}\sqrt{k}\sqrt{a_1^2+b_1^2}\sqrt{\gamma-\mu}\sqrt{\mu+\sigma}}\right), \gamma > \mu. \end{aligned} \tag{15}$$

Finally, the solutions of (6) and (7) are,

$$\begin{aligned} u(x, t) &= -\frac{1}{\sqrt{6}\sqrt{k}\sqrt{a_1^2+b_1^2}\sqrt{\gamma-\mu}\sqrt{\mu+\sigma}}(a_1\sqrt{6ck(\mu+\sigma)-\alpha k^2(\gamma+3\mu+4\sigma)+6\omega(\mu+\sigma)}) \\ &\quad \tanh\left(\frac{c_2(A_0+z)\sqrt{6ck(\mu+\sigma)-\alpha k^2(\gamma+3\mu+4\sigma)+6\omega(\mu+\sigma)}}{\sqrt{6}\sqrt{k}\sqrt{a_1^2+b_1^2}\sqrt{\gamma-\mu}\sqrt{\mu+\sigma}}\right), \quad v(x, t) = \frac{b_1}{a_1}u(x, t) \\ z &= \frac{1}{9\sqrt{ac_2}\sqrt{k(\mu-\gamma)}\sqrt{\mu+\sigma}}(4\alpha k^2t(\gamma+\sigma)^2-3k(\mu+\sigma)(2ct(\gamma+\sigma)+3x(\gamma-\mu)) \\ &\quad +3t\omega(\mu+\sigma)(\gamma-3\mu-2\sigma))\sqrt{a_1^2+b_1^2}. \end{aligned} \tag{16}$$

The solutions in (15) are used to calculate $Re w(x, t)$ which is evaluated numerically and the results are shown in Fig. 1(i)–(iv).

In Fig 1 (i), $Re w(x, t)$ is displayed against x for different values of t when $\mu = 1.1, \gamma = 2.5, \sigma = 0.8$. $Re w(x, t)$ is displayed against t by varying μ when $\gamma = 2.5, \sigma = 0.8$ in Fig. 1(ii).

In Fig. 1(iii), by varying when $\mu = 1.1, \sigma = 0.8$. and in Fig. 1(iv) by varying σ when $\mu = 1.1, \gamma = 2.5$. Together, when $x = -3$.

Figure 1(i) shows pulses compression with quasi SPM Fig. 1(ii), shows the behavior when varying the coefficient of SS towards high values μ .

This figure consolidates the occurrence of self-steepening and we think that pulses progress to shock wave at a value of $\mu = \mu_{cr}$.

Figure 1(iii) shows Raman scattering effect, while Fig. (iv) shows again self-steepening with raising the coefficient of self-phase modulation.

3.1.2 When $r = 2$ and $k = 2$

We consider (12) with AE,

$$g'(z) = g(z) \sqrt{c_2 g(z)^2 + c_1 g(z) + c_0}. \tag{17}$$

From (12) and (17) into (8) and (9) gives rise to,

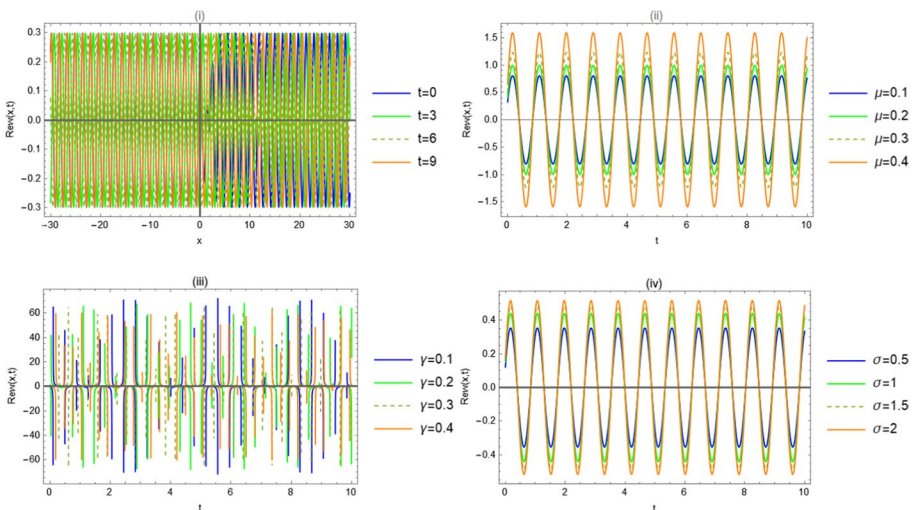


Fig. 1 (i)–(iv) When $c = 0.7, \omega = 7, k = 4, \alpha = 0.7, a_1 = 1.7, b_1 = 1.3, c_2 = 1, A_0 = -10$.

$$\beta = -\frac{(a_1^2+b_1^2)(\gamma-3\mu-2\sigma)}{6c_2h^2}, \quad a_0 = \frac{a_1c_1}{4c_2}, \quad c_0 = \frac{c_1^2}{4c_2}$$

$$d = \frac{1}{48hc_2^2} (a_1^2(8c_2(c_0h^2 - 3k^2) - 3c_1^2h^2)(\gamma - 3\mu - 2\sigma) + 48c_2^2h^2(c - 2\alpha k) + (b_1^2(8c_2(c_0h^2 - 3k^2) - 3c_1^2h^2)(\gamma - 3\mu - 2\sigma))), \tag{18}$$

$$h = \frac{\sqrt{k}\sqrt{a_1^2+b_1^2}\sqrt{\mu+\sigma}}{\sqrt{a}\sqrt{c_2}}, \quad \omega = \frac{1}{48c_2^2(\mu+\sigma)} (k(3a_1^2c_1^2(\gamma - \mu)(\mu + \sigma) + 3b_1^2c_1^2(\gamma - \mu)(\mu + \sigma) + 8c_2^2(\alpha k(\gamma + 3\mu + 4\sigma) - 6c(\mu + \sigma)))).$$

Finally the solutions of (6) and 7 are,

$$u(x, t) = -\frac{a_1c_1\left(2A_0c_2e^{\frac{c_1z}{2\sqrt{c_2}}} + 1\right)}{4c_2\left(2A_0c_2e^{\frac{c_1z}{2\sqrt{c_2}}} - 1\right)}, \quad v(x, t) = \frac{b_1}{a_1}u(x, t),$$

$$z = -\frac{1}{48ac_2c_2^2} (a_1^4c_1^2kt(\mu + \sigma)(\gamma - 3\mu - 2\sigma) + b_1^4c_1^2kt(\mu + \sigma)(\gamma - 3\mu - 2\sigma) + 24b_1^2c_2^2kt(\alpha k(\gamma + \mu + 2\sigma) - 2c(\mu + \sigma)) + 2kta_1^2(b_1^2c_1^2(\mu + \sigma)(\gamma - 3\mu - 2\sigma) + 12 + 12c_2^2(\alpha k(\gamma + \mu + 2\sigma) - 2c(\mu + \sigma))) - 48\sqrt{a}\sqrt{c_2}c_2^2\sqrt{kx}\sqrt{a_1^2 + b_1^2}\sqrt{\mu + \sigma}). \tag{19}$$

The solutions in (19) are used to display $Rew(x, t)$ in Fig. 2 (i)–(iv).

In Fig. 2 (i), $Rew(x, t)$ is displayed against x for different values of t when $\mu = 1.1, \gamma = 2.5, \sigma = 0.8$,

$Rew(x, t)$ is displayed against t by varying μ when $\gamma = 2.5, \sigma = 0.8$ in Fig. 2 (ii).

In Fig. 2(iii) by varying γ when $\mu = 1.1, \sigma = 0.8$, and by varying σ in Fig. 2 (iv) when $\mu = 1.1, \gamma = 2.5$, and when $x = -3$.

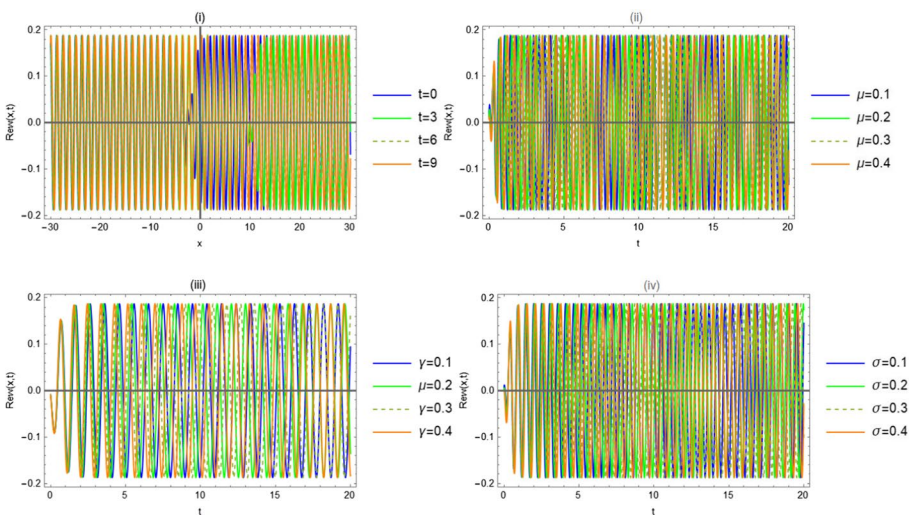


Fig. 2 (i)–(iv). When $c = 0.7, \omega = 7, k = 5, \alpha = 0.7, a_1 = 1.7, b_1 = 1.3, A_0 = -10, c_2 = 2, c_1 = 0.7$.

Figure 2 (i) shows pulses compression with quasi-self-phase modulation on $x > 0$. Fig. 2 (ii) shows also wave compression of shock waves. Fig. 2 (iii) exhibits the extra dispersion effect while Fig. 2 (iv) shows SPM.

3.2 Rational solutions

We write the solutions, when $r = 2$ and $k = 2$, in the form,

$$U(z) = \frac{a_1 g(z) + a_0}{s_1 g(z) + s_0}, \quad V(z) = \frac{b_1 g(z) + b_0}{s_1 g(z) + s_0}, \quad b_0 = \frac{a_0 b_1}{a_1}, \tag{20}$$

together with AE,

$$g'(z) = g(z) \sqrt{-b^2 g(z)^2 + a^2}. \tag{21}$$

From (20) and (21) into (8) and (9) yields,

$$\begin{aligned} \beta &= \frac{(m-1)(\gamma-3\mu-2\sigma)(a_0^2 m^2 s_1^2 + b_1^2 s_0^2)}{3a^2 h^2 m^2 s_0^2 s_1^2}, \quad a_1 = \frac{m(a_0 s_1)}{s_0}, \quad s_1 := \frac{\sqrt{2} b s_0}{\sqrt{a^2(m+1)}}, \\ \omega &= \frac{a^2 h^2 m^2 a s_0^2}{3(m-1)^2 (\mu + \sigma)^2 (a^2 b_1^2 (m+1) + 2a_0^2 b^2 m^2)^2} (6a_0^2 b^2 c 3(m-1)m^2(\mu + \sigma) \\ &\quad + a^2 (2a^2 b^2 h^2 m^2 s_0^2 + 3b_1^2 c 3(m^2 - 1)(\mu + \sigma))), \\ d &= h \left(\frac{a^2 b_1^2 (m^2 + 3m + 2)(\mu + \sigma)}{3b^2 m^2 s_0^2} + \frac{2a_0^2 (m+2)(\mu + \sigma)}{3s_0^2} + c \right. \\ &\quad \left. + \frac{a^2 a^2 b^2 h^2 m^2 s_0^2}{(m-1)(\mu + \sigma)(a^2 b_1^2 (m+1) + 2a_0^2 b^2 m^2)} \right), \\ k &= -\frac{a^2 a b^2 h^2 m^2 s_0^2}{(m-1)(\mu + \sigma)(a^2 b_1^2 (m+1) + 2a_0^2 b^2 m^2)}, \quad \gamma := \mu. \end{aligned} \tag{22}$$

The solution of (21) is,

$$g(z) = \frac{a \operatorname{sech}(a(A_0 + z))}{b}. \tag{23}$$

The solutions of (6) and (7) are,

$$\begin{aligned} u(x, t) &= \frac{a_0 (\sqrt{a^2(m+1)} + \sqrt{2} a \operatorname{sech}(a(A_0 + z)))}{s_0 (\sqrt{a^2(m+1)} + \sqrt{2} a \operatorname{sech}(a(A_0 + z)))}, \quad v(x, t) = \frac{b_1}{a_1} u(x, t), \\ z &= h \left(x + t \left(\frac{a^2 b_1^2 (m^2 + 3m + 2)(\mu + \sigma)}{3b^2 m^2 s_0^2} + \frac{2a_0^2 (m+2)(\mu + \sigma)}{3s_0^2} + c 3 \right. \right. \\ &\quad \left. \left. + \frac{a^2 a^2 b^2 h^2 m^2 s_0^2}{(m-1)(\mu + \sigma)(a^2 b_1^2 (m+1) + 2a_0^2 b^2 m^2)} \right) \right). \end{aligned} \tag{24}$$

The solutions in (24) are used to display $Rew(x, t)$ in Fig. 3 (i)–(vi).

In Fig 3 (i), $Rew(x, t)$ is displayed against x for different values of t when $\mu = 1.1, \sigma = 1.8$.

In Fig 3(ii) and Fig 3(iii) $Rew(x, t)$ is displayed against t by varying μ when $\sigma = 1.8$ and by varying σ when

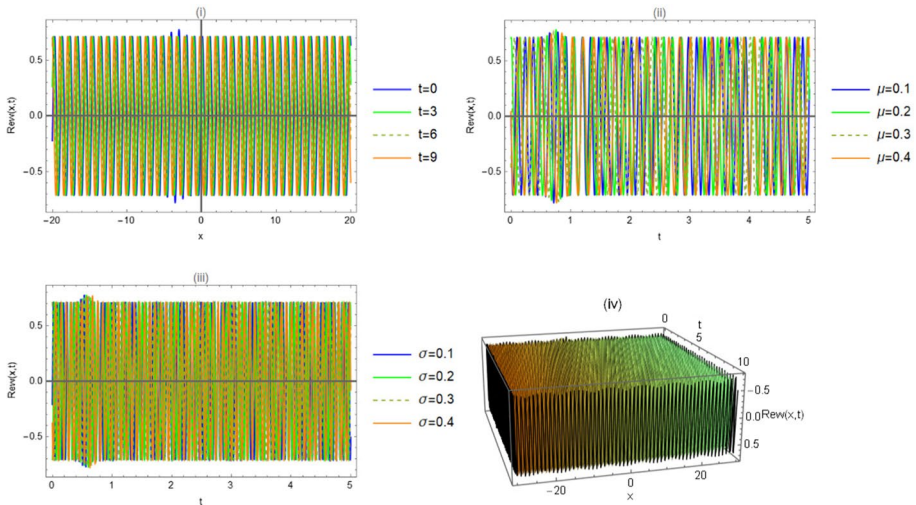


Fig. 3 (i)–(iv). When
 $c = 0.7, \alpha = 0.7, \beta = 0.6, a_0 = 2.7, b_1 = 2.3, h = 1.5, m = 1.2, A_0 = 5, s_0 = 5, a = 1.5, b = 1.3$

$\mu = 1.1$ and when $x = -10$. In Fig. 3 (iv) the 3D plot is displayed for the same values as in Fig. 3(i).

Figure 3(i) show pulses compression, while Fig. 3(ii) and 3(iii) show quasi SPM. These figures show , almost, shock waves. .

4 Elliptic solutions

In this case in (10) and (11), we take $r = 2$. Here, also, polynomial and rational solutions are found.

4.1 Polynomial solutions

4.1.1 When $p = 2$ and $k = 2$

We consider two cases.

Case (I)

We consider (12) with the AE,

$$g'(z) = \sqrt{c_4 g(z)^4 + c_2 g(z)^2 + c_0}. \tag{25}$$

By inserting (12) and (20) into (8) and (9), we have,

$$\beta = -\frac{(a_1^2 + b_1^2)(\gamma - 3\mu - 2\sigma)}{6c_4h^2}, d = \frac{c_2h(a_1^2 + b_1^2)(\gamma - 3\mu - 2\sigma)}{6c_4} - \frac{k^2(a_1^2 + b_1^2)(\gamma - 3\mu - 2\sigma)}{2c_4h} + ch - 2\alpha hk,$$

$$k = \frac{\alpha c_4 h^2}{(a_1^2 + b_1^2)(\mu + \sigma)}, \omega = \frac{h^2 \alpha}{6(a_1^2 + b_1^2)^2(\mu + \sigma)^3} (-3a_1^4 c_2(\gamma - \mu)(\mu + \sigma)^2 - 3b_1^4 c_2(\gamma - \mu)(\mu + \sigma)^2 - 6a_1^2(\mu + \sigma)^2(b_1^2 c_2(\gamma - \mu) + c_4 c) - 6b_1^2 c_4 c(\mu + \sigma)^2 + \alpha^2 c_4^2 h^2(\gamma + 3\mu + 4\sigma)), a_0 = 0.$$
(26)

In (18), we remark that $c_i, i = 0, 2, 4$ are arbitrary. We consider the case when $c_4 = -m^2, c_2 = 2m^2 - 1, c_0 = m^2 - 1$

In this case $g(z) = \text{cn}(z + A_0|m)$ and the solutions of (6) and (7) are,

$$u(x, t) = a_1 \text{cn}(z + A_0|m), v(x, t) = b_1 \text{cn}(z + A_0|m),$$

$$z = t \left(-\frac{\alpha^2 c_4 h^3 (\gamma - 3\mu - 2\sigma)}{2(a_1^2 + b_1^2)(\mu + \sigma)^2} - \frac{2\alpha^2 c_4 h^3}{(a_1^2 + b_1^2)(\mu + \sigma)} + \frac{c_2 h (a_1^2 + b_1^2)(\gamma - 3\mu - 2\sigma)}{6c_4} + ch \right) + hx.$$
(27)

By using (27), $\text{Re}w(x, t)$ is displayed in figures 4 (i)–(iv).

In Fig 4 (i), $\text{Re}w(x, t)$ is displayed against x for different values of t when $\gamma = 2.5, \mu = 1.1, \sigma = 0.8$.

In Fig. 4(ii), (iii) and (iv), $\text{Re}w(x, t)$ is displayed against t for different values of μ when $\gamma = 2.5, \sigma = 0.8$,

against γ when $\mu = 1.1, \sigma = 0.8$, and against σ when $\gamma = 2.5, \mu = 1.1$, respectively and when $x = 3$.

Figure 4(i) shows chirped waves. Fig. 4(ii) shows highly dispersive waves induced by the the extra dispersion.

While Fig. 4 (ii) and (iv) show highly oscillatory pulses with SPM.

Case (II)

Here consider (12) with the AE,

$$g'(z) = \sqrt{c_2 g(z)^2 + c_1 g(z) + c_0} \sqrt{r_2 g(z)^2 + r_1 g(z) + r_0}. \tag{28}$$

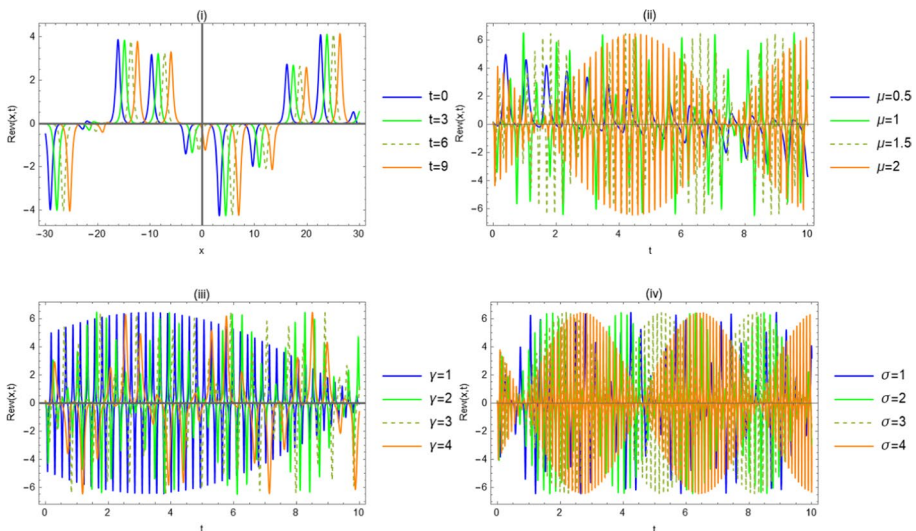


Fig. 4 (i)–(iv). When $k = 4, \alpha = 0.7, a_1 = 3.7, b_1 = 5.3, m = 0.999, h = 3, A_0 = -5, c = 0.7$.

By inserting (12) and (28) gives rise to,

$$\begin{aligned}
 h &= \frac{\sqrt{a_1^2 + b_1^2} \sqrt{-\gamma + 3\mu + 2\sigma}}{\sqrt{6} \sqrt{\beta} \sqrt{c_2} \sqrt{r_2}}, \quad a_0 = \frac{1}{4} a_1 \left(\frac{c_1}{c_2} + \frac{r_1}{r_2} \right), \\
 d &= \frac{\sqrt{a_1^2 + b_1^2} \sqrt{-\gamma + 3\mu + 2\sigma}}{48 \sqrt{6} \sqrt{\beta} c_2^{5/2} r_2^{5/2}} (8c_2^2 r_0 r_2 (a_1^2 + b_1^2) (\gamma - 3\mu - 2\sigma) \\
 &\quad + 8c_0 c_2 r_2^2 (a_1^2 + b_1^2) (\gamma - 3\mu - 2\sigma) + 8c_1 c_2 r_1 r_2 (a_1^2 + b_1^2) (\gamma - 3\mu - 2\sigma) \\
 &\quad + 48c_2^2 c_3 r_2^2 - 3(a_1^2 + b_1^2) (c_2 r_1 + c_1 r_2)^2 (\gamma - 3\mu - 2\sigma) + 144\beta c_2^2 k^2 r_2^2 - 96\alpha c_2^2 k r_2^2), \\
 k &= \frac{\alpha(-\gamma + 3\mu + 2\sigma)}{6\beta(\mu + \sigma)}, \quad \omega = \frac{\alpha(\gamma - 3\mu - 2\sigma)}{216\beta^2 c_1 r_2^2 (\mu + \sigma)^3} (-9a_1^2 \beta c_1 r_1^2 (\gamma - \mu)(\mu + \sigma)^2 \\
 &\quad - 18a_1^2 \beta c_1 r_0 r_2 (\gamma - \mu)(\mu + \sigma)^2 + 9\beta b_1^2 c_1 r_1^2 (\gamma - \mu)(\mu + \sigma)^2 + 18\beta b_1^2 c_1 r_0 r_2 \\
 &\quad (\gamma - \mu)(\mu + \sigma)^2 + 18a_1^2 \beta c_0 r_1 r_2 (\gamma - \mu)(\mu + \sigma)^2 + 18\beta b_1^2 c_0 r_1 r_2 (\gamma - \mu)(\mu + \sigma)^2 \\
 &\quad + \alpha^2 c_1 r_2^2 (\gamma - 3\mu - 2\sigma)^2 + 36\beta c_1 c_3 r_2^2 (\mu + \sigma)^2 + 6\alpha^2 c_1 r_2^2 (\mu + \sigma)(\gamma - 3\mu - 2\sigma)), \\
 c_2 &= \frac{c_1 r_2}{r_1}.
 \end{aligned} \tag{29}$$

The solution of (28) is,

$$g(z) = - \frac{\sqrt{r_1^2 - 4r_0 r_2} \operatorname{sn} \left(\frac{1}{2} (z + A_0) \sqrt{c_1 r_1 - 4c_0 r_2} \Big| \frac{c_1 (r_1^2 - 4r_0 r_2)}{r_1 (c_1 r_1 - 4c_0 r_2)} \right) + r_1}{2r_2}. \tag{30}$$

Finally the solutions of (6) and (7) are,

$$\begin{aligned}
 u(x, t) &= - \frac{a_1 \sqrt{r_1^2 - 4r_0 r_2} \operatorname{sn} \left(\frac{1}{2} (z + A_0) \sqrt{c_1 r_1 - 4c_0 r_2} \Big| \frac{c_1 (r_1^2 - 4r_0 r_2)}{r_1 (c_1 r_1 - 4c_0 r_2)} \right)}{2r_2}, \\
 v(x, t) &= \frac{b_1}{a_1} u(x, t), \\
 z &= \frac{c_1 \sqrt{a_1^2 + b_1^2} \sqrt{-\gamma + 3\mu + 2\sigma}}{12 \sqrt{6} \sqrt{\beta} \sqrt{r_2} \left(\frac{c_1 r_2}{r_1} \right)^{5/2}} \left(\frac{12c_1 r_2^2 x}{r_1^2} + t (c_1 (a_1^2 + b_1^2) (-\gamma - 3\mu - 2\sigma)) \right. \\
 &\quad + \frac{2c_1 r_0 r_2 (a_1^2 + b_1^2) (\gamma - 3\mu - 2\sigma)}{r_1^2} + \frac{2c_0 r_2 (a_1^2 + b_1^2) (\gamma - 3\mu - 2\sigma)}{r_1} \\
 &\quad \left. + \frac{12c_1 c_3 r_2^2}{r_1^2} + \frac{4\alpha^2 c_1 r_2^2 (\gamma - 3\mu - 2\sigma)}{\beta r_1^2 (\mu + \sigma)} + \frac{\alpha^2 c_1 r_2^2 (\gamma - 3\mu - 2\sigma)^2}{\beta r_1^2 (\mu + \sigma)^2} \right). \tag{31}
 \end{aligned}$$

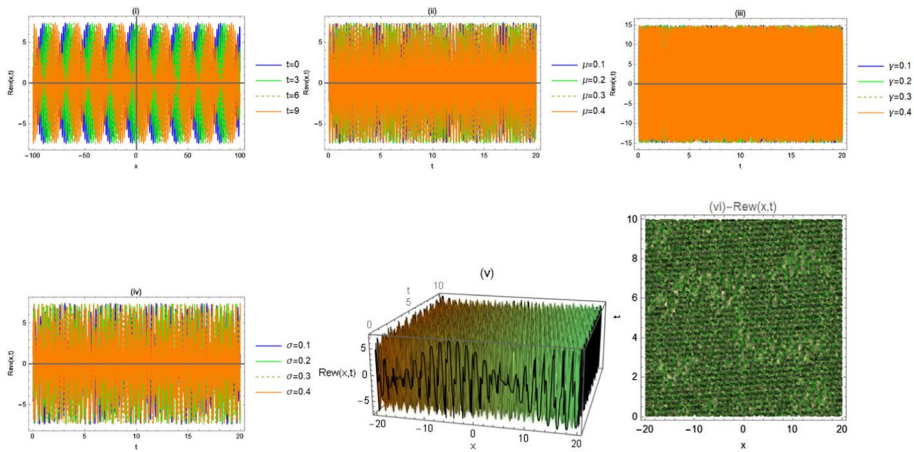


Fig. 5 (i)–(iv). When $\omega = 7, k = 4, \alpha = 0.7, a_1 = 1.7, b_1 = 1.3, c_0 = 1.2, r_1 = 2.3, r_0 = 0.5, r_2 = 0.3,$

The results in (31) are evaluated numerically and $Rew(x, t)$ is shown in Fig. 5 (i)–(vi).
 $c_1 = 3.3, \beta = 1.2, A_0 = 4, c = 0.7.$

In Fig. 5(i), $Rew(x, t)$ is displayed against x for different values of t when $\gamma = 2.5, \mu = 1.1, \sigma = 0.8, .$

In Fig. 5(ii), (iii) and (iv) , $Rew(x, t)$ is displayed against t for different values of μ when $\gamma = 2.5, \sigma = 1.8. , \gamma$ when $\mu = 1.1, \sigma = 1.8,$ and σ when $\gamma = 2.5, \mu = 1.1.$ respectively when $x = 3.$

In Fig. 5 (v) and (vi) the 3D and contour plots are displayed for the same values in Fig. 5(i).

Figure 5(i) shows quasi-self-phase modulation. Fig. 5 (ii) shows more narrower waves than in

Figure 5(i), for a small value of μ which corresponds to self-steepening effect.

Fig. 5 (iii) shows scattered dense pulses compression, while Fig. 5(iv) show highly dispersive waves which may be argued to the presence of the extra dispersion.

Fig. 5 (v) shows quasi-self-phase modulation, while Fig. 5 (vi) shows lattice wave.

4.2 Rational solutions

Now, we consider (20) together with the AE,

$$g'(z) = \sqrt{c_4 g(z)^4 + c_2 g(z)^2 + c_0}. \tag{32}$$

From (20) and (32) into (8) and (9) yields,

$$\begin{aligned}
 \omega &= \frac{a_0^2 k (a_1^2 + b_1^2) (\gamma - \mu)}{a_1^2 s_0^2} + \frac{2 a_1 c_0 h^2 s_0 s_1 (\alpha - 3 \beta k)}{a_0 s_0^2} \\
 &\quad - \frac{2 c_0 h^2 s_1^2 (\alpha - 3 \beta k)}{s_0^2} - k (c_3 + \beta k^2 - \alpha k), \\
 \beta &:= \frac{-2 a_0^3 k (a_1^2 + b_1^2) (\gamma - \mu) + \alpha a_1^2 a_0 h^2 (c_2 s_0^2 + 4 c_0 s_1^2) + 2 \alpha a_1^3 c_0 h^2 s_0 s_1}{3 a_1^2 h^2 k (2 a_1 c_0 s_0 s_1 + a_0 (c_2 s_0^2 + 4 c_0 s_1^2))}, \quad a_0 = -\frac{a_1 s_0}{s_1}, \\
 c_0 &= \frac{c_4 s_0^4}{s_1^4}, \quad d = \frac{1}{3 h k s_1^2 (2 c_4 s_0^2 + c_2 s_1^2)} (-h^2 2 c_4 s_0^2 + c_2 s_1^2 (6 \alpha c_4 h^2 s_0^2 \\
 &\quad + (\alpha c_2 h^2 + 3 k (\alpha k - c_3) s_1^2)) + k a_1^2 (6 c_4 h^2 s_0^2 (\gamma + \mu + 2 \sigma) \\
 &\quad + (6 k^2 (\mu - \gamma) + h^2 (-\gamma + 7 \mu \\
 &\quad + 6 \sigma) c_2) s_1^2) + b_1^2 k (s_1^2 (c_2 h^2 (-\gamma + 7 \mu + 6 \sigma) + 6 k^2 (\mu - \gamma)) \\
 &\quad + 6 c_4 h^2 s_0^2 (\gamma + \mu + 2 \sigma))), \\
 k &= \frac{\alpha h^2 (2 c_4 s_0^2 + c_2 s_1^2)}{4 (a_1^2 + b_1^2) (\mu + \sigma)}, \quad c_2 = -m^2.
 \end{aligned} \tag{33}$$

The solution of (32) is,

$$\begin{aligned}
 g(z) &= \frac{\sqrt{2} \left(s_1^2 \left(m^2 \sqrt{m^4 s_1^4 - 4 c_4^2 s_0^4} - m^4 s_1^2 \right) + 2 c_4^2 s_0^4 \right)}{\sqrt{c_4 s_1^4} \left(m^2 s_1^2 - \sqrt{m^4 s_1^4 - 4 c_4^2 s_0^4} \right)^{3/2}} \\
 &\quad \operatorname{sn} \left(\frac{(A_0 + z) \left(\sqrt{2 c_4 s_0^2} \right)}{\sqrt{m^2 s_1^2 - \sqrt{m^4 s_1^4 - 4 c_4^2 s_0^4}}} \middle| \frac{m^2 s_1^2 - \sqrt{m^4 s_1^4 - 4 c_4^2 s_0^4}}{\sqrt{m^4 s_1^4 - 4 c_4^2 s_0^4} + m^2 s_1^2} \right).
 \end{aligned} \tag{34}$$

The solutions of (6) and (7) are,

$$\begin{aligned}
 u(x, t) &= \frac{\frac{a_1}{s_1} (-\sqrt{c_4 s_0 s_1^4} \left(m^2 s_1^2 - \sqrt{m^4 s_1^4 - 4 c_4^2 s_0^4} \right)^{3/2} + s_1 H)}{\sqrt{c_4 s_1^3 s_0} \left(m^2 s_1^2 - \sqrt{m^4 s_1^4 - 4 c_4^2 s_0^4} \right)^{3/2} + H}, \quad v(x, t) = \frac{b_1}{a_1} u(x, t), \\
 H &= \sqrt{2} \left(m^2 s_1^2 \sqrt{m^4 s_1^4 - 4 c_4^2 s_0^4} + 2 c_4^2 s_0^4 - m^4 s_1^4 \right) \operatorname{sn} \left(\frac{\sqrt{2} (z + A_0) c_4 s_0^2}{\sqrt{m^2 s_1^2 - \sqrt{m^4 s_1^4 - 4 c_4^2 s_0^4}}} \middle| \frac{m^2 s_1^2 - \sqrt{m^4 s_1^4 - 4 c_4^2 s_0^4}}{m^2 s_1^2 + \sqrt{m^4 s_1^4 - 4 c_4^2 s_0^4}} \right).
 \end{aligned} \tag{35}$$

The solutions in (35) are used to display $Rew(x, t)$ in Fig. 6 (i)–(vi).

In Fig 6 (i), $Rew(x, t)$ is displayed against x for different values of t when $\gamma = 2.5, \mu = 1.1, \sigma = 1.8$.

$Rew(x, t)$ is displayed against t for different values of μ , when $\gamma = 2.5, \sigma = 1.8$ in Fig. 6(ii), against γ when $\mu = 1.1, \sigma = 1.8$ in

Figure 6(iii) and against σ , when $\gamma = 2.5, \mu = 1.1$ in Fig. 6(iv), and when $x = -10$.

In Fig. 6 (v) and (vi) the 3D and contour plots are displayed for the same values in Fig. 5(i).

Figure 6(i) shows SPM interaction. Fig. 5 (ii) shows that self-steepening holds for small values of μ .

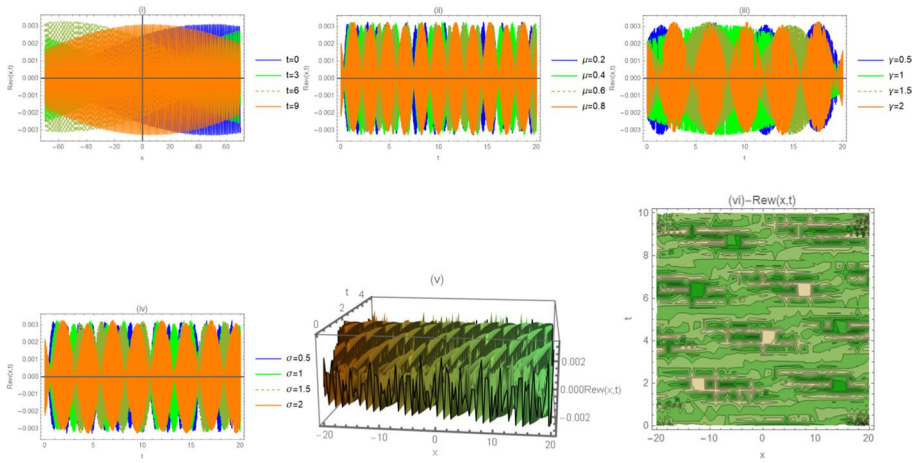


Fig. 6 (i)–(iv) When
 $m = 0.5, n = 0.75, c_2 = -m^2, A_0 = -5, s_1 = 5, c = 0.7, \alpha = 0.7, \beta = 0.6, a_1 = 1.7, b_1 = 1.3, h = 0.8.$

Fig. 6 (iii) shows SPM-RS interaction, while Fig. 5(iv) show dispersive waves due to the extra dispersion.

Fig 6 (v) shows complex chirped waves, while Fig. 6 (vi) shows lattice wave.

5 Modulation instability and spectral analysis

5.1 Modulation instability

The study of modulation instability (MI) holds in a system which posses normal mode solution. This occurs for systems with complex envelope field. In Eq. (4), it has a solution of the form,

$$w(x, t) = Ae^{i(Kx-t\Omega)}, \quad w^*(x, t) = Ae^{-i(Kx-t\Omega)}, A \in \mathbb{R}. \tag{36}$$

The solution in (36) holds when,

$$\Omega = -cK + \alpha K^2 - \beta K^3 + \gamma K - K\mu. \tag{37}$$

Noe, we use the perturbation expansion,

$$\begin{aligned} w(x, t) &= e^{i(Kx-t\Omega)} \left(A + e^{\lambda t} (\epsilon_1 U_1(x) + i\epsilon_2 V_1(x)) \right), \\ w^*(x, t) &= e^{-i(Kx-t\Omega)} \left(A + e^{\lambda t} (\epsilon_1 U_1(x) - i\epsilon_2 V_1(x)) \right). \end{aligned} \tag{38}$$

From (38) into (4) gives rise to,

$$\begin{aligned}
 H \begin{pmatrix} \epsilon_1 \\ \epsilon_2 \end{pmatrix} &= 0, \quad H = \begin{pmatrix} h_{11} & h_{12} \\ h_{21} & h_{22} \end{pmatrix}, \\
 h_{11} &= U_1(x)(3A^2K(\mu - \gamma) + cK - \alpha K^2 + \beta K^3 + \Omega) + (\alpha - 3\beta K)U_1''(x), \\
 h_{21} &:= V_1'(x)(A^2(\mu - \gamma) + c + 3\beta K^2 - 2\alpha K) - \beta V_1^{(3)}(x) + \lambda(-V_1(x)), \\
 h_{12} &= -U_1'(x)(A^2(-(\gamma - 3\mu)) + c + 3\beta K^2 - 2\alpha K) + \lambda U_1(x) - + U_1^{(3)}(x), \\
 h_{22} &:= V_1(x)(A^2K(\mu - \gamma) + cK - \alpha K^2 + \beta K^3 + \Omega) + (\alpha - 3\beta K)V_1''(x).
 \end{aligned} \tag{39}$$

The solution of (39) is $\det(H) = 0$, which yields a lengthy equation which will not produced her. It describes the eigenvalue problem. This equation is solved when subjected to boundary conditions (BCs) . Here, we assume that $U(\pm\infty) = -0$ and $V(\pm\infty) = -0$. The BCs suggest to write the solutions,

$$\begin{pmatrix} U(x) \\ V(x) \end{pmatrix} = \begin{pmatrix} A_1 \\ A_2 \end{pmatrix} \begin{cases} e^{-rx}, & r > 0, x > 0, \\ e^{rx}, & x < 0. \end{cases} \tag{40}$$

By inserting (40) into the eigenvalue equation, we get,

$$\begin{aligned}
 A_2((3A^4 - 4A^2 + 1)K^2(\gamma - \mu)^2 + 2(2A^2 - 1)Kr^2(\gamma - \mu)(3\beta K - \alpha) + r^4(\alpha - 3\beta K)^2) \\
 - A_1(r(-A^2(\gamma - 3\mu) + 3\beta K^2 - 2\alpha K) + cr + \lambda + r^3)^2 = 0,
 \end{aligned} \tag{41}$$

Which solves to,

$$\begin{aligned}
 \lambda &= \frac{1}{A_1}(-A_1cr - A_1r^3 + 2\alpha A_1Kr - 3A_1\beta K^2r + A^2A_1\gamma r - 3A^2A_1\mu r + \sqrt{\Delta}), \\
 \Delta &= A_1B_1((3A^4 - 4A^2 + 1)K^2(\gamma - \mu)^2 + 2(2A^2 - 1)Kr^2(\gamma - \mu)(3\beta K - \alpha) \\
 &\quad + r^4(\alpha - 3\beta K)^2).
 \end{aligned} \tag{42}$$

The MI does not depend on the sign of Δ and it holds when,

$$\mu > \frac{\gamma(A^2\gamma - c - 3\beta K^2 + 2\alpha K - r^2)}{3A^2}, \quad \gamma > \frac{c + 3\beta K^2 - 2\alpha K + r^2}{A^2}. \tag{43}$$

That is when $\mu > \mu_{cr}$ and $\gamma > \gamma_{cr}$.When MI occurs, it triggers, SS , shock waves and RS effect is produced.

5.2 Spectral analysis

Here we define the average wave number and the frequency and the spectrum content,

$$\bar{k} = \frac{\iint_{\mathbb{R} \times \mathbb{R}^+} |w(x, t)_x| dx dt}{\iint_{\mathbb{R} \times \mathbb{R}^+} |w(x, t)| dx dt}, \quad \bar{\omega} = \frac{\iint_{\mathbb{R} \times \mathbb{R}^+} |w(x, t)_t| dx dt}{\iint_{\mathbb{R} \times \mathbb{R}^+} |w(x, t)| dx dt}. \tag{44}$$

The spectral content is defined by,

$$W(k, t) = \frac{1}{2\pi} \left| \int_{\mathbb{R}} e^{-ikx} w(x, t) dx \right|. \tag{45}$$

Here, by using (44) and (45), we illustrate the spectral analysis of the solutions in (16). This is demonstrated in Fig. 7(i)–(iv).

$$c := 0.7, \omega:7, k = 4; \alpha := 0.7, a_1 = 1.7, b_1 = 1.3, c_2 = 1, A_0 = -10.$$

In Fig. 7 (i) $\gamma = 2.5, \sigma = 1.8$ In Fig. 7(ii) $\mu = 0.5, \sigma = 0.8$

In Fig. 7(iii) $\mu = 0.5, \gamma = 0.9$. The same hold in Fig. 7(iv)–(vi). In Fig. 7(vii) $\gamma = 2.5, \mu = 0.5, \sigma = 0.8$

In Fig. 7(i)–(iii) the wave number is displayed. In Fig. 7 (iv)–(vi) the frequency is displayed. The spectrum is shown in Fig. 7(vii).

After Fig. 7 (i)–(vi), we the values of k and $\bar{\omega}$ do not vary significantly when varying the parameters μ, γ and σ .

Figure 7(vii) shows that the spectrum exhibits soliton with periodic waves background.

6 Conclusions

The perturbed Chen–Lee–Liu equation with third order dispersion is studied for the objective of investigating the effects of the self-steepening, Raman scattering, self -phase modulation, and the extra dispersion on the configuration of pulses propagation in optical fibers. This is inspected via the exact solutions, which are found by using the unified method. The results obtained are evaluated numerically and the are represented in figures which demonstrate the behavior of the solutions with relevance with the aforementioned phenomena. Also, it is found that self phase modulation occurs currently. While self-steepening is triggered by modulation instability. Also, highly dispersive oscillatory waves are observed which may be argued to the presence of an extra dispersion. These results are new. Further, pulses compression are, also, currently remarked. The modulation instability is studied and it is established that when it holds, it triggers self-steepening which progresses to shock waves. It is remarked that the wave spectrum exhibits soliton with background periodic

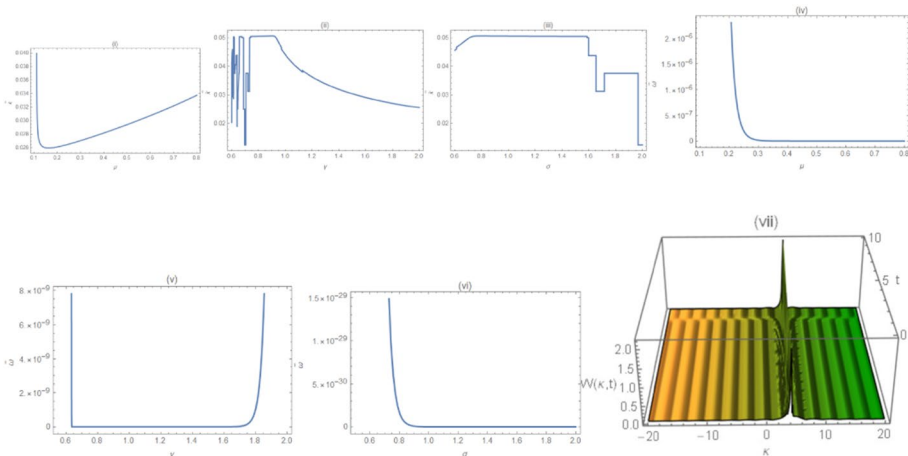


Fig. 7 (i)–(vii). When $c = 0.7, \omega:7, k = 4; \alpha := 0.7, a_1 = 1.7, b_1 = 1.3, c_2 = 1, A_0 = -10$.

waves. In a future work, the perturbed Chen–Lee–Liu equation with time dependent coefficients will be studied.

Funding Open access funding provided by The Science, Technology & Innovation Funding Authority (STDF) in cooperation with The Egyptian Knowledge Bank (EKB).

Open Access This article is licensed under a Creative Commons Attribution 4.0 International License, which permits use, sharing, adaptation, distribution and reproduction in any medium or format, as long as you give appropriate credit to the original author(s) and the source, provide a link to the Creative Commons licence, and indicate if changes were made. The images or other third party material in this article are included in the article's Creative Commons licence, unless indicated otherwise in a credit line to the material. If material is not included in the article's Creative Commons licence and your intended use is not permitted by statutory regulation or exceeds the permitted use, you will need to obtain permission directly from the copyright holder. To view a copy of this licence, visit <http://creativecommons.org/licenses/by/4.0/>.

References

- Abdel-Gawad, H.I.: Towards a unified method for exact Solutions of evolution Equations. An application to reaction diffusion equations with finite memory transport. *J. Stat. Phys.* **147**, 506–521 (2012)
- Abdel-Gawad, H.I.: Chirped, breathers, diamond and W-shaped optical waves propagation in non self-phase modulation medium. Biswas–Arshed equation. *Int. J. Mode. Phys. B* **35**(7), 2150097 (2021a)
- Abdel-Gawad, H.I.: Study of modulation instability and geometric structures of multi solitons in a medium with high dispersivity and nonlinearity. *Pramana J. Phys.* **95**, 146 (2021b)
- Abdel-Gawad, H. I.: A generalized Kundu–Eckhaus equation with an extra-dispersion: pulses configuration. *Opt. Quant. Electron.* **53** (2021c)
- Abdel-Gawad, H. I.: Inelastic soliton interactions for nonlinear directional couplers in optical metamaterials with Kerr nonlinearity modulation stability. *J. Nonlinear Opt. Phys. Mater.* (2021d). <https://doi.org/10.1142/S0218863522500163>
- Abdel-Gawad, H.I.: The eigenvalue problem of the general Einstein-Weyl metric equation and exact self-similar and multi-traveling waves solutions. *Indian J. Phys.* **96**, 473–479 (2022)
- Abdel-Gawad, H. I., Tantawy, M., Fahmy, I. S., Park, C.: Langmuir waves trapping in a (1+2) dimensional plasma system. Spectral and modulation stability analysis. *Chin. J. Phys.* (2022). <https://doi.org/10.1016/j.cjph.2022.01.018>
- Abdelkawy, M.A., Ezz-Eldien, S.S., Biswas, A., Alzahrani, K., Belic, M.R.: Optical solitons for Chen–Lee–Liu equation with two spectral collocation approaches. *Comput. Math. Math. Phys.* **61**, 1432–1443 (2021)
- Akram, G., Mahak, N.: Traveling wave and exact solutions for the perturbed nonlinear Schrodinger equation with Kerr law nonlinearity. *Eur. Phys. J. Plus* **133**, 212 (2018)
- Alrashed, R., Alshaery, A.A., Alkhatee, S.: Optical solitons via the collective variable method for the classical and perturbed Chen–Lee–Liu equations. *Open Phys.* (2021). <https://doi.org/10.1515/phys-2021-0065>
- Bansal, A., Biswas, A., Zhou, Q., Arshed, S., Alzahrani, A. K., Belic, M. R.: Optical solitons with Chen–Lee–Liu equation by Lie symmetry. *Phys.Lett. A* **384**(10), 126202 (2020)
- Bilal, M., Hu, W., Ren, J.: Different wave structures to the Chen–Lee–Liu equation of monomode fibers and its modulation instability analysis. *Eur. Phys. J. Plus* **136**, 385 (2021)
- Chen, H.H., Lee, Y.C., Liu, C.S.: Integrability of nonlinear Hamiltonian systems by inverse scattering method. *Phys. Scr.* **20**(3–4), 490 (1979)
- Dépélaire, B., Gambo, B.E., Nsangou, M.: Effects of fractional temporal evolution on chirped soliton solutions of the Chen–Lee–Liu equation, *Phys. Scr.* **96**, 105215 (2021)
- Gao, W., Ghanbari, B., Günerhan, H., Baskonus, H. M.: Some mixed trigonometric complex soliton solutions to the perturbed nonlinear Schrödinger equation. *Mod. Phys. Lett. B* **34**(03), 2050034 (2020)
- Gaxiola, O.G., Biswas, A.: W-shaped optical solitons of Chen–Lee–Liu equation by Laplace–Adomian decomposition method. *Opt Quant Electron* **50**, 314 (2018)
- Houwe, A., Abbagari, S., Almohsen, B., Betchewe, G., Inc, M., Doka, S.Y.: Chirped solitary waves of the perturbed Chen–Lee–Liu equation and modulation instability in optical monomode fibres. *Opt. Quant. Electron.* **53**, 286 (2021)

- Ivanov, S.K.: Riemann problem for the light pulses in optical fibers for the generalized Chen–Lee–Liu equation. *Phys. Rev. A* **101**, 053827 (2021)
- Karaa, A.H., Biswas, A., Zhou, Q., aMorarue, L., Moshoko, S. P., Belic, M.: Conservation laws for optical solitons with Chen–Lee–Liu equation. *Optik* **174**, 195–198 (2018)
- Kudryashov, N.A.: General solution of the traveling wave reduction for the perturbed Chen–Lee–Liu equation. *Optik* **186**, 339–349 (2019)
- Liu, C., Wu, Y.-H., Chen, S.-C., Yao, X., Akhmediev, N.: Exact analytic spectra of asymmetric modulation instability in systems with self-steepening effect. *Phys. Rev. Lett.* **127**, 094102 (2021)
- Ma, W.-X.: N-soliton solution and the Hirota condition of a (2+1)-dimensional combined equation. *Math. Comput. Simul.* **190**, 270–279 (2021)
- Ma, W.-X.: Riemann–Hilbert problems and inverse scattering of nonlocal real reverse-spacetime matrix AKNS hierarchies. *Physica D* **430**, 133078 (2022)
- Ma, W.-X., Yong, X.: Xing LiuSoliton solutions to the B-type Kadomtsev–Petviashvili equation under general dispersion relations. *Wave Motion* **103**, 102719 (2021)
- Mahak, N., Akram, G.: Extension of rational sine-cosine and rational sinh-cosh techniques to extract solutions for the perturbed NLSE with Kerr law nonlinearity. *Eur. Phys. J. Plus* **134**, 159 (2019)
- Martínez, H. Y., Rezazadeh, H., Inc, M., Akinlar, M. A.: New solutions to the fractional perturbed Chen–Lee–Liu equation with a new local fractional derivative. *Waves Rand. Complex Med.* (2021). <https://doi.org/10.1080/17455030.2021.1930280>
- Miah, M.M., Ali, H.M.S., Akbar, M.A.: An investigation of abundant traveling wave solutions of complex nonlinear evolution equations: the perturbed nonlinear Schrödinger equation and the cubic–quintic Ginzburg–Landau equation. *Cogent. Math.* **3**(1) (2016)
- Mihalache, D., Torner, L., Moldoveanu, F.: N -C Panoiu and N Truta, Soliton solutions for a perturbed nonlinear Schrödinger equation. *J. Phys. A* **26**, L757 (1993)
- Mohamed, M.S., Akinyemi, L., Najati, S.A., Elagan, S.K.: Abundant solitary wave solutions of the Chen–Lee–Liu equation via a novel analytical technique. *Opt. Quant. Electron.* **54**, 141 (2022)
- Neirameh, A.: New soliton solutions to the fractional perturbed nonlinear Schrödinger equation with power law nonlinearity. *SeMA* **73**, 309–323 (2016)
- Osman, M.S., Almusaw, H., Tariq, K. U., Anwar, S., S. Kumar, M., Younis, Ma, W.-X.: On global behavior for complex soliton solutions of the perturbed nonlinear Schrödinger equation in nonlinear optical fibers, *J. Ocean Eng. Sci.* (2021). <https://doi.org/10.1016/j.joes.2021.09.018>
- Sarla, S., Ali, K.K., Yilmazer, R., Osman, M.S.: New optical solitons based on the perturbed Chen–Lee–Liu model through Jacobi elliptic function method. *Opt. Quant. Electron.* **54**, 131 (2022)
- Shehata, M.S.M.: A new solitary wave solution of the perturbed nonlinear Schrödinger equation using a Riccati–Bernoulli Sub-ODE method. *Int. J. Phys. Sci.* **11**(6), 80–84 (2016)
- Tantawy, M., Abdel-Gawad, H.I.: On multi-geometric structures optical waves propagation in self-phase modulation medium: Sasa–Satsuma equation. *Eur. Phys. J. Plus* **135**, 928 (2020)
- Yokuş, A., Durur, H., Duran, H.S.: Simulation and refraction event of complex hyperbolic type solitary wave in plasma and optical fiber for the perturbed Chen–Lee–Liu equation. *Opt. Quant. Electron.* **53**, 402 (2021)
- Yıldırım, Y.: Optical solitons to Chen–Lee–Liu model in birefringent fibers with trial equation approach. *Optik* **183**, 881–886 (2019)
- Yıldırma, Y., Biswas, A., Asma, M., Ekici, M., Ntsime, B.P., Zayed, E.M.E., Moshokoai, S.P., Alzahrani, A.K., Belic, M.R.: Optical soliton perturbation with Chen–Lee–Liu equation. *Optik* **220**, 165177 (2020)
- Zhang, Z.-Y., Liu, Z.-H., Miao, X.J., Chen, Y.-Z.: New exact solutions to the perturbed nonlinear Schrödinger's equation with Kerr law nonlinearity. *Appl. Math. Comput.* **216**(100), 3064–3072 (2010)
- Zhang, P. J., Liu, W., Qiu, D., Zhang, Y.i., Porsezian, K., Jingsong, H.: Rogue wave solutions of a higher-order Chen–Lee–Liu equation. *Phys. Scr.* **90**, 055207 (2015)
- Zhou, Q.: Analytical solutions and modulation instability analysis to the perturbed nonlinear Schrödinger equation. *J. Mod. Phys.* **61**(6) (2014)